N-(5-Fluoro-2-phenoxyphenyl)-*N*-(2-[^{131}I]iodo-5-methoxybenzyl)acetamide: A Potent Iodinated Radioligand for the Peripheral-type Benzodiazepine Receptor in Brain

Ming-Rong Zhang,*[,†] Katsushi Kumata,[†] Jun Maeda,[‡] Terushi Haradahira,[†] Junko Noguchi,[†] Tetsuya Suhara,[‡] Christer Halldin,[§] and Kazutoshi Suzuki[†]

Radiochemistry Section, Department of Molecular Probe, Molecular Imaging Center, National Institute of Radiological Sciences, 4-9-1 Anagawa, Inage-ku, Chiba 263-8555, Japan, Molecular Neurobiology Section, Department of Molecular Neuroimaging, Molecular Imaging Center, National Institute of Radiological Sciences, 4-9-1 Anagawa, Inage-ku, Chiba 263-8555, Japan, and Psychiatry Section, Department of Clinical Neuroscience, Karolinska Institute, S17176 Stockholm, Sweden

Received September 28, 2006

To image the peripheral-type benzodiazepine receptor (PBR) in vivo, we previously developed two positron emission tomography (PET) ligands, *N*-(2-[^{11}C],5-dimethoxybenzyl)-*N*-(5-fluoro-2-phenoxyphenyl)acetamide ([^{11}C]**1a**) and its [^{18}F]fluoroethyl analogue ([^{18}F]**1b**), for the investigation of PBR in the living human brain. This time, using **1a** as a leading compound, we designed two novel iodinated analogues, *N*-(5-fluoro-2-phenoxyphenyl)-*N*-(2-iodo-5-methoxybenzyl)acetamide (**3a**) and *N*-(2,5-dimethoxybenzyl)-*N*-(5-iodo-2-phenoxyphenyl)acetamide (**3b**) for the PBR imaging. Ligands **3** were synthesized by the iodination of tributystannyl precursors **10**. Radiolabeling for **3** with ^{131}I was carried out by the reaction of **10** with [^{131}I]-NaI using H_2O_2 as an oxidizing agent. In vitro competition experiments determined that **3a** exhibited both high affinity and selectivity for PBR (IC_{50}: 7.8 nM) vs CBR (>1 μM). Biodistribution study in mice determined that [^{131}I]**3a** had a high radioactivity level (1.69% dose/g) in the brain, and its distribution pattern in the brain was consistent with the known distribution of PBR in rodents. Ex vivo autoradiography of the rat brain gave visual evidence that [^{131}I]**3a** was a potent and specific radioligand for PBR.

Introduction

The peripheral-type benzodiazepine receptor (PBR),[1] which is an 18-kDa protein as a critical functional unit of a multimeric 140−200-kDa complex,[2] is mainly distributed in the outer mitochondrial membrane at the cellular level.[3,4] PBR, which was initially identified in the peripheral tissues, was also found in the central nervous system (CNS).[5] In the CNS, PBR is mainly located in glial cells, which are distributed in the olfactory bulb and cerebellum of rodents, and in the occipital cortex, etc., of primates.[6−10] It has been demonstrated that glial cells play a crucial role in neurodegenerative process in the CNS.[11] When a brain was injured, glial cells in the brain were activated, which led to increased PBR receptor density;[12] therefore, PBR has been determined as a sensitive marker protein for activated glial cells in various experimental models of brain injury.[12−14] So far, clinical investigations for PBR have revealed that this receptor correlates with various brain injuries[12−14] and neurodegenerative disorders such as Alzheimer's disease[15−17] and multiple sclerosis.[18,19] These findings have prompted the development of radioligands for PBR, which can be used to visualize this receptor and to measure its level in vivo in both humans and animals.[20−24]

Recently, we have developed two novel PET ligands: *N*-(2-[^{11}C], 5-dimethoxybenzyl)-*N*-(5-fluoro-2-phenoxyphenyl)-acetamide ([^{11}C]DAA1106, [^{11}C]**1a**, Scheme 1) and *N*-(5-fluoro-2-phenoxyphenyl)-*N*-(2-[^{18}F]fluoroethoxy-5-methoxybenzyl)-acetamide ([^{18}F]FEDAA1106, [^{18}F]**1b**) for PBR imaging.[25−27] The two ligands had more potent in vitro binding affinities for PBR than 1-(2-chlorophenyl)-*N*-methyl,*N*-(1-methylpropyl)-isoquinoline (PK11195, **2a**), a standard ligand for PBR, and had remarkable selectivity against other receptors including the classical central benzodiazepine receptor (CBR).[27−29] In vivo study determined that [^{11}C]**1a** and [^{18}F]**1b** had higher uptake and better specific binding in rodent and primate brains than [^{11}C]PK11195 ([^{11}C]**2a**).[25−27] Now, [^{11}C]**1a** and [^{18}F]**1b** are being used to investigate PBR in human brains in our laboratory to elucidate the relationship between PBR and brain diseases.[31,32]

In addition to PET, single photoemission computed tomography (SPECT) is another radioimaging modality for in vivo investigation and diagnosis. Although PET provides functional information with higher resolution and better selectivity than SPECT, SPECT imaging is a more practical and routine method for clinical usefulness due to the convenient production of radiopharmaceuticals. So far, several radioiodinated ligands for PBR imaging have been developed and evaluated in rodents and primates.[33−35] Of these ligands, [^{123}I]**2b**, an iodinated

Table 1. In Vitro Binding Affinity (IC_{50}) for Peripheral Benzodiazepine Receptor (PBR) and Central Benzodiazepine Receptor (CBR), and Octanol/Phosphate Buffer Distribution Coefficient (logD)

			IC_{50} (nM)[a]			
			PBR			
ligand	R_1	R_2	for [^{11}C]**1a**[b]	**for [^{11}C]2a**[b]	CBR[c]	logD[d]
3a	F	I	7.8 ± 0.4	4.4 ± 0.1	>10000	4.42
3b	I	OCH_3	69.2 ± 5.9	60.1 ± 6.3	>10000	4.03
1a (DAA1106)			1.6 ± 0.1	1.3 ± 0.7	>10000	3.65
2a (PK11195)			8.3 ± 1.2	9.2 ± 0.4	>10000	2.78

[a] Values (mean ± SD) represent the mean obtained from nine concentrations of compound using at least eight slices of rat brain ($n = 3$). [b] [^{11}C]1a and [^{11}C]2a were incubated in the presence of the compounds examined, respectively. [c] [^{11}C]Flumazenil was incubated in the presence of the compounds examined. [d] The logD values were determined in the phosphate buffer (pH = 7.4)/octanol system using the shaking flask method. All results were presented as mean values ($n = 3$) with a maximum range of ±5%.

* Corresponding author. Tel: 81-43-206-4041; Fax: 81-43-206-3261; E-mail: zhang@nirs.go.jp.

[†] Department of Molecular Probes, National Institute of Radiological Sciences.

[‡] Department of Molecular Neuroimaging, National Institute of Radiological Sciences

[§] Karolinska Institute.

10.1021/jm061127n CCC: $37.00 © 2007 American Chemical Society
Published on Web 01/11/2007

Scheme 1. Chemical Structures of DAA1106 (**1**) and PK11195 (**2**) Analogues

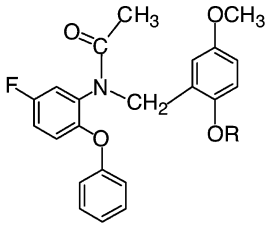

DAA1106 (**1a**): R = CH_3
[^{11}C]DAA1106 ([^{11}C]**1a**): R = $^{11}CH_3$
FEDAA1106 (**1b**): R = FCH_2CH_2
[^{18}F]FEDAA1106 ([^{18}F]**1b**): R = $^{18}FCH_2CH_2$

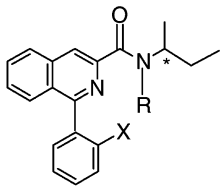

PK 11195 (**2a**): R = CH_3, X = Cl
[^{11}C]PK11195 ([^{11}C]**2a**): R = $^{11}CH_3$, X = Cl
[^{123}I]PK11195 ([^{123}I]**2b**): R = CH_3, X = ^{123}I

Scheme 2. Chemical Structures of Iodinated Analogues **3a** and **3b**

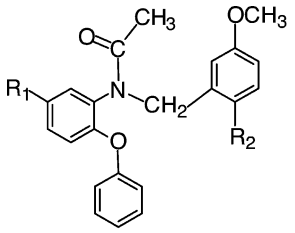

3a: R_1 = F, R_2 = I
[^{131}I]**3a**: R_1 = F, R_2 = [^{131}I]I
3b: R_1 = I, R_2 = OCH_3
[^{131}I]**3b**: R_1 = [^{131}I]I, R_2 = OCH_3

analogue of **2a** (Scheme 1), has been used for the assessment of neuroinflammation and microglial activation in Alzheimer's disease.[17]

Here, using **1a** as a lead compound, we designed two novel iodinated ligands: *N*-(5-fluoro-2-phenoxyphenyl)-*N*-(2-iodo-5-methoxybenzyl)acetamide (**3a**) and *N*-(2,5-dimethoxybenzyl)-*N*-(5-iodo-2-phenoxyphenyl)acetamide (**3b**) (Scheme 2). These compounds could be labeled not only by the gamma emitter ^{123}I for SPECT, but also by the positron emitter ^{124}I for PET and other radioiodines without changing their chemical structures and pharmacological profiles. In this paper, we report the (1) chemical synthesis of **3a** and **3b** starting from commercial materials, (2) radiolabeling of **3a** and **3b** using easily handled ^{131}I, and (3) in vitro binding affinity to PBR and biodistribution of these ligands in rodent brains.

Chemistry. The synthetic route chosen for the preparation of ligands **3a** and **3b** involved introduction of the iodine onto the benzene ring by the iodination of tributylstannyl precursors. They were prepared in a six-step sequences of reactions delineated in Scheme 3, respectively. In this synthetic approach, the reactions of 2-bromonitrobenzenes **4** with phenol under basic conditions afforded 2-phenoxynitrobenzenes **5**, which were reduced with powdered iron and then treated with acetyl chloride to give acetanilides **7**. Alkylations of **7** with benzyl halides **8** using sodium hydride as a base afforded bromoacetanilides **9**, which were treated with bistributyltin in the presence of tetrakis-(triphenyphosphine)palladium (0) to give tributylstannyl precursors **10**. The stannylation of **9a** to form **10a** required much longer reaction time (90 h) than that of **9b** to form **10b** (18 h). This difference relates steric hindrance in **9a** to restricted rotation of the benzyl group as inferred form the two signals for its methylene protons in ^{1}H NMR spectrum. Finally, the desired products **3a** and **3b** were prepared by iodination of the tributylstannyl **10** with iodine powder. The two reactions proceeded rapidly even at room temperature to afford **3** at high chemical yields of >80%, respectively.

The labeling of **3a** and **3b** using ^{131}I was carried out as shown in Scheme 3. The [^{131}I]iodination of the tributylstannyl precursor **10a** or **10b** with [^{131}I]NaI was performed by regioselective destannylation under mild reaction conditions using H_2O_2 as an oxidizing agent in acetic acid. After the reaction was completed, the radioactive mixture was applied onto a semi-preparative HPLC system with a radioactive detector. Within 8−11 min of starting HPLC purification, the radioactive fraction corresponding to [^{131}I]**3a** or [^{131}I]**3b** was collected and the solvents were removed by nitrogen gas flow at room temperature. The obtained residue was redissolved in saline containing 10% ethanol to give the desired radioactive product as an intravenously injectable solution. Using HPLC and radio-TLC, the identity of [^{131}I]**3** was confirmed by comparison with the non-radioactive **3**, and the radiochemical purity in the products was determined to be >98%, respectively. The specific activity of [^{131}I]**3** was assumed to >30 GBq/μmol based on the specific activity of the commercial [^{131}I]NaI. In the final products, no significant chemical impurities were determined. Moreover, the radiochemical purity of [^{131}I]**3** remained >95% after maintenance of the products at room temperature for 24 h, and they were stable for performing the evaluation on animals.

In Vitro Binding Assays. The in vitro binding affinities (IC_{50}) of ligands **3a** and **3b** for PBR were determined from competition against [^{11}C]**1a** and [^{11}C]**2a** binding to PBR by using quantitative autoradiography[27] on rat brain sections. As shown in Table 1, replacement of the methoxyl group by an iodine atom onto the benzyl moiety maintained the potency of **3a** for PBR. Although the binding affinity of **3a** (IC_{50}: 7.8 nM for [^{11}C]**1a** or 4.4 nM for [^{11}C]**2a**) was slightly lower than that of **1a** (1.6 nM or 1.3 nM), **3a** showed a similar potency with **2a** (8.3 nM or 9.2 nM), the mostly used standard ligand for PBR. This result suggests that the electron density and size of the substitution group in the benzene ring of the benzyl could not affect interaction between PBR and **3a** significantly. This finding was in agreement with our previous results that replacement of the methoxyl group (**1a**) by several alkoxyl groups such as OCH_2F, OCD_2F, OCH_2CH_2F (**1b**), OCH_2CH_3, and $OCH(CH_3)_2$ groups could maintain their binding affinities for PBR.[24,27] Contrary to **3a**, substitution of the fluorine with an iodine atom onto the acetanilide weakened the binding affinity of **3b** for PBR. The affinity of **3b** was 40-, 8-, and 10-fold lower than those of **1a**, **2a**, and **3a**, respectively. The iodine bulky in the benzene ring of acetanilide appeared unfavorable for expressing the affinity for PBR, despite the some similarity of iodine and fluorine atoms. This finding suggests that the conformation of **3b** while interacting with PBR was affected negatively due to iodine hindrance. Considering that these

Scheme 3. Chemical Synthesis and Radiosynthesis

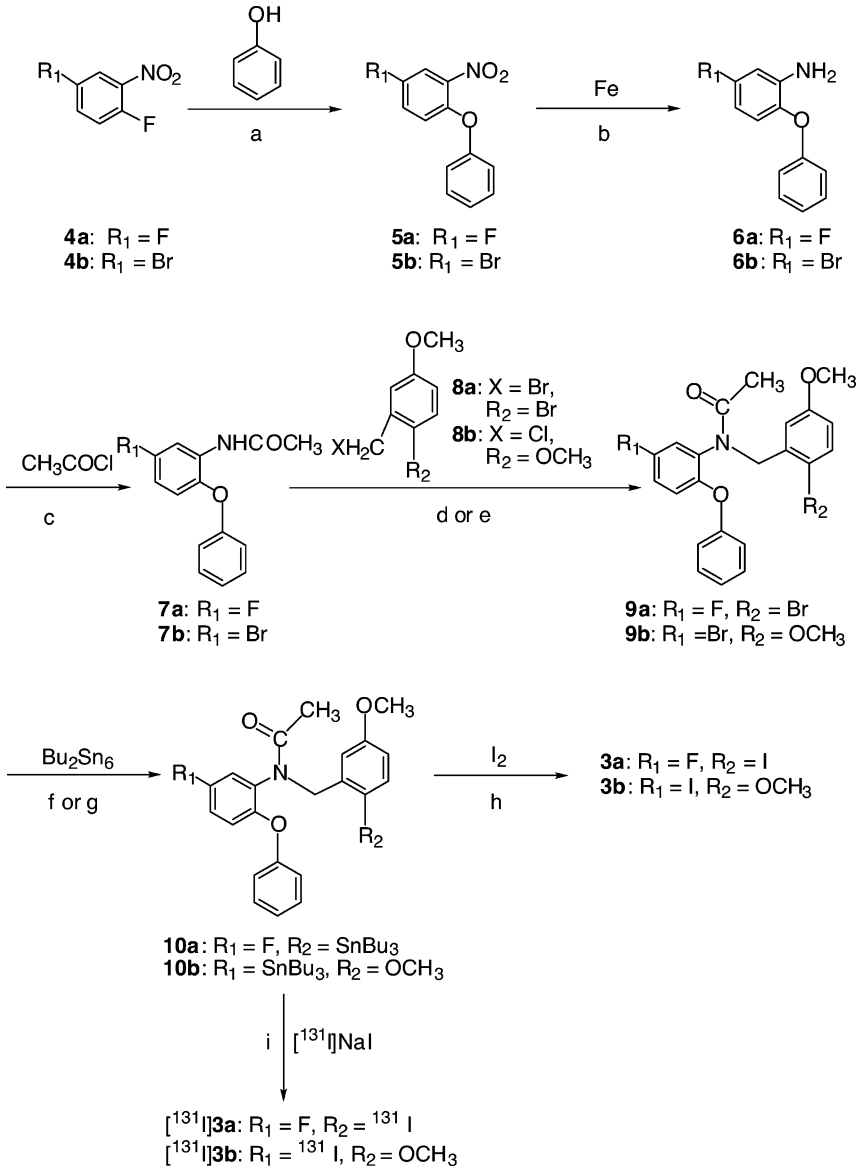

(a)K_2CO_3, DMF, 80 °C, 3 h; b) NH_4Cl, EtOH, H_2O, 80 °C, 5 h; (c) Et_3N, CH_2Cl_2, room temperature, 3 h; (d) NaH, DMF, room temperature, 6 h; (e) NaH, DMF, room temperature, 3 h; (f) $Pd(PPh_3)_4$, toluene, reflux, 90 h; (g) $Pd(PPh_3)_4$, toluene, reflux, 18 h; (h) CH_2Cl_2, 25 °C, 3 h; (i) H_2O_2, AcOH, EtOH, 25 °C, 30 min.

derivatives evolved from the classical benzodiazepine structure, the in vitro binding affinities of **3a** and **3b** for the central benzodiazepine receptor (CBR) were measured by competition against the CBR-selective [^{11}C]flumazenil binding. As can be seen in Table 1, the two ligands did not display remarkable inhibitory effects (IC_{50}>1 μM) on the [^{11}C]flumazenil binding in the rat brain. Their high selectivity for PBR over CBR may be due to their drastically structural difference from the classical benzodiazepine ring. The in vitro binding experiment demonstrated that **3a** had both high affinity and selectivity for PBR vs CBR.

Brain Uptake in Mice. The uptake of [^{131}I]**3a** and [^{131}I]**3b** was examined in mouse brains and the radioactivity levels are expressed as percent dose per gram of tissue weight (% dose/g) as shown in Table 2. [^{131}I]**3a** showed a rapid penetration into the brain and exhibited high initial uptake (1.06% dose/g) in the entire brain at 1 min after intravenous injection. At 15 min after injection, the uptake of [^{131}I]**3a** reached the maximum value (1.69% dose/ g) and then displayed gradual washout from the brain over 60 min. After 60 min, the brain uptake (0.75% dose/g) had decreased 44% when compared to the uptake at 15 min. The result suggests that this ligand does pass across the brain−blood barrier (BBB) into the brain, which is a prerequisite for a promising radioligand for brain imaging. This finding was also compatible with its high lipophilicity expressed as a distribution coefficient (logD: 4.42), as shown in Table 1.

The regional distribution of [^{131}I]**3a** in the mouse brains was determined over 60 min (Table 2). The radioactivity of [^{131}I]**3a** accumulated with time in all regions examined, and the uptake in these regions peaked during 15−30 min and then declined until 60 min. Among the brain regions examined, the highest uptake (3.06% dose/g at 15 min) was observed in the olfactory bulb, the highest PBR density area in the mouse brain. Following the olfactory bulb, a high radioactivity level (2.32% dose/g at 15 min) was also detected in the cerebellum, whereas a moderate or low uptake was observed in the cerebral cortex, hypothalamus, thalamus, striatum, and hippocampus. The uptake pattern of radioactivity was consistent not only with [^{3}H]**1a**[28]

Table 2. Brain Regional Distribution (% Injected Dose/g Tissue: Mean ± SD, $n = 3$) of [^{131}I]**3a** and [^{131}I]**3b** in Mice at 1, 5, 15, 30, 60 min after Injection

ligand	tissue	1 min	5 min	15 min	30 min	60 min
3a	whole brain	1.06 ± 0.25	1.38 ± 0.32	1.69 ± 0.21	1.28 ± 0.44	0.75 ± 0.17
	cerebellum	1.21 ± 0.49	1.48 ± 0.38	2.32 ± 0.28	1.63 ± 0.24	1.00 ± 0.12
	olfactory bulb	1.49 ± 0.51	2.24 ± 0.34	3.06 ± 0.39	2.42 ± 0.43	1.17 ± 0.56
	hippocampus	0.53 ± 0.21	0.62 ± 0.49	0.75 ± 0.32	0.59 ± 0.26	0.55 ± 0.21
	striatum	0.71 ± 0.15	0.71 ± 0.23	0.69 ± 0.24	0.60 ± 0.31	0.23 ± 0.16
	cerebral cortex	0.82 ± 0.26	0.91 ± 0.35	0.84 ± 0.26	0.55 ± 0.12	0.24 ± 0.09
	hypothalamus	0.78 ± 0.18	0.99 ± 0.34	0.97 ± 0.18	0.73 ± 0.29	0.41 ± 0.13
	thalamus	0.67 ± 0.20	0.49 ± 0.10	0.48 ± 0.25	0.53 ± 0.16	0.32 ± 0.07
	blood	2.34 ± 0.89	1.85 ± 0.23	1.11 ± 0.46	0.76 ± 0.35	0.25 ± 0.24
3b	whole brain	0.87 ± 0.39	1.15 ± 0.36	0.71 ± 0.30	0.38 ± 0.12	0.18 ± 0.17
	cerebellum	0.92 ± 0.45	1.08 ± 0.24	0.79 ± 0.09	0.44 ± 0.06	0.16 ± 0.08
	olfactory bulb	1.15 ± 0.34	1.35 ± 0.29	1.02 ± 0.51	0.58 ± 0.13	0.24 ± 0.12
	hippocampus	0.25 ± 0.15	0.67 ± 0.41	0.37 ± 0.25	0.23 ± 0.17	0.08 ± 0.13
	striatum	0.47 ± 0.17	0.46 ± 0.05	0.55 ± 0.22	0.26 ± 0.19	0.12 ± 0.14
	cerebral cortex	0.60 ± 0.12	0.48 ± 0.32	0.36 ± 0.23	0.13 ± 0.30	0.16 ± 0.09
	hypothalamus	0.22 ± 0.06	0.39 ± 0.03	0.45 ± 0.10	0.21 ± 0.22	0.21 ± 0.19
	thalamus	0.53 ± 0.04	0.61 ± 0.08	0.35 ± 0.19	0.20 ± 0.01	0.14 ± 0.02
	blood	2.67 ± 1.01	1.99 ± 0.58	1.38 ± 0.51	0.41 ± 0.38	0.29 ± 0.20

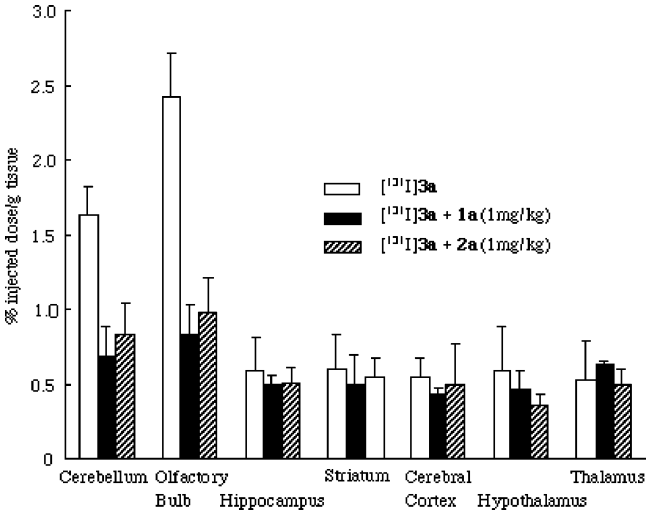

Figure 1. Effects of the PBR-selective **1a** (1 mg/kg) and **2a** (1 mg/kg) on [^{131}I]**3a** concentrations (mean ± SD, $n = 3$) in selected regions of mouse brains at 30 min after intravenous injection (0.4 MBq).

and [^{11}C]**1a**[25,26] binding sites in the rat or mouse brain, but also with the known regional distribution of PBR in the rodent brain.[6,7]

On the other hand, although [^{131}I]**3b** had rapid and high initial uptake into the brain, its radioactivity peaked (1.15% dose/g) at 5 min after injection, which was 67% of [^{131}I]**3b**. From 5 min, [^{131}I]**3b** displayed a gradual washout of radioactivity from various regions. At 15 min after injection, the radioactivity of [^{131}I]**3b** in the mouse brain had decreased by 0.91% dose/g (54% of [^{131}I]**3a** at the same time point). Moreover, the highest levels of radioactivity for [^{131}I]**3b** in the olfactory bulb and cerebellum were 33% and 30% of those for [^{131}I]**3a**, respectively. The relatively lower uptake of [^{131}I]**3b** in the brain was due to lower in vitro binding affinity with PBR. Although **3b** was also highly lipophilic (logD: 4.03), its binding affinity was >10 fold lower than that of **3a**. These results demonstrated that [^{131}I]**3b** did not display a more favorable property as a ligand for PBR imaging in the brain than [^{131}I]**3a**, therefore, no further evaluation of [^{131}I]**3b** was carried out.

The in vivo specificity of [^{131}I]**3a** for PBR was tested by co-injecting PBR-selective **1a** and **2a** at a dose of 1 mg/kg body weight, respectively. The result of the blocking study at 30 min after injection is presented in Figure 1. Co-injection with nonradioactive **1a** reduced the radioactivity of [^{131}I]**3a** in the brain regions compared with the control group. The most significant decrease was found in the olfactory bulb (33% of control) and cerebellum (40% of control). Other brain regions (striatum, hippocampus, hypothalamus, and cerebral cortex) showed slow decreases (60−90%) in the percent uptake of [^{131}I]-**3a**. The inhibition experiment determined that some specific bindings of [^{131}I]**3a** occurred in the all brain regions, and high levels (>60% of total binding) were present in the olfactory bulb and cerebellum. PBR-selective **2a** (1 mg/kg) also significantly reduced radioactivity in these regions of the mouse brain, to an extent similar to that obtained using the same amount of **1a**. The largest decrease in the radioactivity occurred in the olfactory bulb (40%) and cerebellum (48%) compared with the control group. These results indicate that the uptake of radioactivity in PBR-rich regions after the injection of [^{131}I]**3a** was due to PBR sites in the mouse brain. Moreover, [^{131}I]**3a** exhibited potentially favorable kinetic properties for the in vivo imaging of PBR in the brain.

Ex Vivo Autoradiography. The ex vivo autoradiography technique cannot only provide visual evidence of radioligand binding with a receptor, but also afford statistical information about ligand distribution in the regions of interest (ROI). Figure 2 (a) shows an ex vivo autoradiogram of [^{131}I]**3a** for the rat brain at 30 min after intravenous injection. This image revealed the relatively high radioactivity level of [^{131}I]**3a** in the rat brain, as detected in the mouse brain. Among the regions examined, the highest radioactivity was observed in the choroids plexus,[26,28] which is a structure related to the secretion of cerebrospinal fluid containing a large concentration of PBR. In addition, a high level of radioactivity was also seen in the olfactory bulb. Following the olfactory bulb, moderate radioactivity was detected in the cerebellum, whereas low uptake was detected in other regions such as the cerebral cortex and striatum. The distribution order reflected the known distribution of PBR in the rodent brain. In the previous studies, autoradiograms of [^{3}H]-**1a**[26] and [^{11}C]**1a**[28] also demonstrated that a high density of PBR binding is localized in the olfactory bulb and choroids plexus.[6,7] Quantitative analysis was performed for all autoradiograms ($n = 15$) obtained from the rat brain. The radioactivity in each brain region was determined and expressed as a photostimulated-luminescence (PSL)/mm^2 region. As shown in Figure 2 (c), using the striatum as a reference region with low PBR density,[28] the ratios of choroids plexus and olfactory bulb to the striatum were 3.2 and 1.5, respectively, for [^{131}C]**3a**, whereas the ratios of other brain regions to the striatum were about 1.0−1.5. These

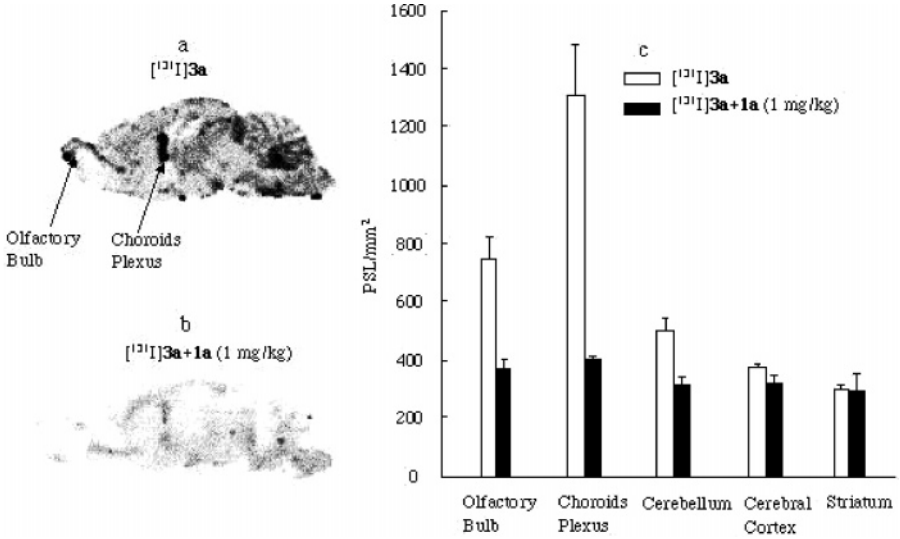

Figure 2. Ex vivo autoradiograms of [^{131}I]**3a** in the sagittal sections of rat brains at 30 min after injection (2 MBq): (a) [^{131}I]**3a**; (b) [^{131}I]**3a** + **1a** (1 mg/kg); (c) the radioactivity distribution of [^{131}I]**3a** in the brain regions. The radioactivity level in each region was determined from the brain images ($n = 10-15$) and was expressed by as photostimulated-luminescence (PSL)/mm^2 region.

visual results indicate that the uptake of radioactivity in PBR-rich regions after the injection of [^{131}I]**3a** was due to PBR sites in the rat brain.

To further determine the in vivo specificity of [^{131}I]**3a** in the rat brain, a blocking study was performed in which non-radioactive **1a** (1 mg/kg body weight) was injected simultaneously with [^{131}I]**3a**. As shown in Figure 2 (b), PBR-selective **1a** significantly reduced radioactivity in the brain regions. This high dose of **1a** abolished regional differences in the uptake of radioactivity in the olfactory bulb, choroids plexus, and other brain regions. Quantitative analysis of these images ($n = 10$) revealed the most evident decreases in the choroids plexus (43% of the control) and olfactory bulb (43%) (Figure 2 (c)). Other brain regions (cerebellum, striatum, and frontal cortex, etc.) showed moderate or low decreases in the percent uptake (63−85%) of [^{131}I]**3a**. These results further support that high specific binding of [^{131}I]**3a** to PBR occurred in the olfactory bulb and choroids plexus of the rat brain.

The in vivo stability of [^{131}I]**3a** in the mouse brains ($n = 3$) was determined. At 30 min after injection, 90−94% of total radioactivity in the brain homogenate represented unchanged [^{131}I]**3a,** and no significant radioactive metabolites were detected in the brain homogenate. Thus, all specific [^{131}I]**3a** binding determined in the brain might be due to this ligand itself and not influenced by its radioactive metabolites. This result suggests that [^{131}I]**3a** could serve as an in vivo imaging agent for PBR in the brain.

Conclusion

In this study, two novel iodinated compound, **3a** and **3b**, were designed, synthesized, and evaluated for PBR imaging in rodent brains. [^{131}I]**3a** and [^{131}I]**3b** were prepared by no carrier-added [^{131}I]NaI treatment of their corresponding tributylstannyl precursors (**10a** and **10b**) with I^+ generated in situ by H_2O_2 oxidation of $^{131}I^-$. In vitro binding assays for the rat sections determined that **3a** had potent affinity and exhibited high selectivity for PBR over CBR, whereas **3b** was weaker than **3a**. A biodistribution study determined that [^{131}I]**3a** had high uptake in the mouse brain and good specific binding in regions rich in PBR. An ex vivo autoradiography study provided visual evidence that specific binding of [^{131}I]**3a** to PBR occurred in the rat brain.

This study has succeeded in developing a potential iodinated ligand [^{131}I]**3a** which has high specific binding for PBR in rodent brains. This novel ligand can be labeled not only by ^{123}I for SPECT but also by ^{124}I or ^{11}C for PET and then can be evaluated in rodents and primates. These studies are in progress in our laboratory.

Experimental Section

All chemicals and solvents of the highest grade commercially available were purchased from Aldrich Chem. (Milwaukee, WI) and Wako Pure Chem. Ind. (Osaka) without further purification in all cases. The melting points (mp) were determined using a Yanaco MP-500D melting point apparatus and are uncorrected. ^{1}H NMR spectra were recorded on a JNM-GX-300 spectrometer (JEOL, Tokyo) with tetramethylsilane as an internal standard. All chemical shifts (δ) were reported in parts per million (ppm) downfield from the standard. FAB-MS was obtained on a JEOL NMS-SX102 spectrometer (JEOL, Tokyo). Column chromatography was carried out using silica gel (WAKO Wakogel C-200). Thin-layer chromatography analyses (TLC) were performed using silica gel F_{254} PLC plates (20 × 20, 0.5 μm; Merck). Radioactive mixtures were purified and analyzed by high-performance liquid chromatography (HPLC) with an in-line UV (254 nm) detector in series with a NaI crystal radioactivity detector. Isolated radioactivity was measured with an IGC-3 Curiemeter (Aloka, Tokyo). All animal experiments were carried out according to the recommendations of the committee for the care and use of laboratory animals, National Institute of Radiological Sciences (NIRS).

5-Bromo-2-phenoxynitrobenzene (5b). A mixture of 5-bromo-2-fluoronitrobenzene (**4b**; 1.10 g, 5.0 mmol), phenol (0.52 g, 5.5 mmol), and K_2CO_3 powder (0.83 g, 5.0 mmol) in DMF (10 mL) was stirred at 80 °C for 3 h. The mixture was concentrated under reduced pressure, and the residue was partitioned between AcOEt and water. The separated organic layer was washed with 1 M aqueous HCl and saturated NaCl solution. After the organic layer was dried over Na_2SO_4, the solvent was removed to give **5b** (1.44 g, 98%) as a yellowish oil. ^{1}H NMR ($CDCl_3$) δ: 8.08 (1H, d, J = 2.4 Hz), 7.58 (1H, dd, J = 2.4, 8.8 Hz), 7.40 (2H, t, J = 7.7 Hz), 7.21 (1H, t, J = 7.7 Hz), 7.05 (2H, d, J = 7.7 Hz), 6.89 (1H, d, J = 8.8 Hz). HRMS (FAB) Calcd for $C_{12}H_8BrNO_3$: 293.9766. Found: 293.9754.

5-Bromo-2-phenoxyaniline (6b). A mixture of **5b** (1.0 g, 3.4 mmol), Fe powder (0.63 g, 11.0 mmol), and NH_4Cl (91 mg, 1.7 mmol) in a mixture of EtOH (10 mL) and water (3 mL) was stirred at 80 °C for 5 h. The reaction mixture was quenched with AcOEt, and the separated organic layer was washed with water. After the organic layer was dried over Na_2SO_4, the solvent was removed to give **6b** (0.84 g, 94%) as a pale brown solid. Mp: 47−48 °C. ^{1}H

NMR ($CDCl_3$) δ: 7.30 (2H, t, J = 7.9 Hz), 7.07 (1H, t, J = 7.9 Hz), 6.94−6.97 (3H, m), 6.80 (1H, dd, J = 2.2, 8.4 Hz), 6.70 (1H, d, J = 8.4 Hz), 3.85 (2H, br). FABMS (*m/z*): 264 ($M^+ + 1$), 266 ($M^+ + 3$). HRMS (FAB) Calcd for $C_{12}H_{10}BrNO$: 263.9958. Found: 263.9991.

***N*-Acetyl-5-bromo-2-phenoxyaniline (7b)**. To a solution of **6b** (0.70 g, 2.7 mmol) and Et_3N (0.46 mL, 3.3 mmol) in CH_2Cl_2 (6 mL) was added acetyl chloride (0.45 mL, 3.0 mmol) in a dropwise manner under cooling in an ice-bath, and the mixture was stirred at room temperature for 3 h. After the reaction mixture was concentrated under reduced pressure, the residue was quenched with AcOEt and washed with water and a saturated NaCl solution. After the organic layer was dried over Na_2SO_4, the solvent was removed to give a residue. The residue was chromatographed on silica gel with AcOEt/hexane (1/5) to obtain **7b** (0.69 g, 85%) as a pale yellow oil. ^{1}H NMR ($CDCl_3$) δ: 8.66 (1H, d, J = 2.0 Hz), 7.72 (1H, br), 7.38 (2H, t, J = 8.0 Hz), 7.18 (1H, t, J = 7.4 Hz), 7.10 (1H, dd, J = 2.4, 11.0 Hz), 7.01 (2H, d, J = 7.9 Hz), 6.68 (1H, d, J = 8.6 Hz), 2.18 (3H, s). FABMS (*m/z*): 306 ($M^+ + 1$); 308 ($M^+ + 3$). HRMS (FAB) Calcd for $C_{14}H_{12}BrNO_2$: 306.0201. Found: 306.0165.

***N*-(2-Bromo-5-methoxybenzyl)-*N*-(5-fluoro-2-phenoxyphenyl)acetamide (9a)**. To a solution of **7a**[36] (4.52 g, 18.4 mmol) in DMF (20 mL) was added NaH (60% dispersion in mineral oil, 0.80 g, 20 mmol), and the mixture was stirred for 1 h at room temperature. To the mixture was added 2-bromo-5-methoxybenzyl bromide (**8a**; 5.04 g, 18 mmol), which was prepared by reacting 2-bromo-5-methoxytoluene with *N*-bromosuccinimide. The reaction mixture was stirred for 5 h at room temperature. The mixture was poured into ice water and extracted with AcOEt three times. The combined organic layer was washed with 0.5 M aqueous HCl and saturated NaCl solution. After the organic layer was dried over Na_2SO_4, the solvent was removed to give a residue. This residue was chromatographed on silica gel with AcOEt/hexane (1/5) to afford **9a** (5.33 g, 65%) as a yellowish oil. ^{1}H NMR ($CDCl_3$) δ: 7.29−7.31 (3H, m), 7.12 (1H, t, J = 7.3 Hz), 6.92−7.02 (2H, m), 6.81−6.89 (4H, m), 6.62 (1H, d, J = 8.8 Hz), 5.18 (1H, d, J = 15.1 Hz), 4.74 (1H, d, J = 15.1 Hz), 3.66 (3H, s), 2.00 (3H, s). HRMS (FAB) Calcd for $C_{22}H_{19}BrFNO_3$: 444.0520. Found: 444.0565.

***N*-(5-Bromo-2-phenoxyphenyl)-*N*-(2,5-dimethoxybenzyl)acetamide (9b)**. To a solution of **7b** (3.58 g, 11.7 mmol) in DMF (20 mL) was added NaH (60% dispersion in mineral oil, 0.80 g, 20 mmol), and the mixture was stirred for 1 h at room temperature. To this mixture was added 2,5-dimethoxybenzyl chloride (**8b**; 3.02 g, 16.5 mmol), which was prepared by reacting 2,5-dimethoxybenzyl alcohol with concentrated HCl. The reaction mixture was stirred for 2 h at room temperature. The mixture was poured into ice−water and extracted with AcOEt three times. The combined organic layer was washed with 0.5 M aqueous HCl and saturated NaCl solution. After the organic layer was dried over Na_2SO_4, the solvent was removed to give a residue. This residue was chromatographed on silica gel with AcOEt/hexane (1:5) to obtain **9b** (5.06 g, 94.8%) as a white solid. Mp: 118.5−119.5 °C. ^{1}H NMR ($CDCl_3$) δ: 7.29−7.35 (3H, m), 7.12−7.21 (2H, m), 6.95 (1H, d, J = 2.8 Hz), 6.84 (2H, d, J = 7.7 Hz), 6.66−6.75 (3H, m), 5.05 (1H, d, J = 14.3 Hz), 4.73 (1H, d, J = 14.3 Hz), 3.67 (3H, s), 3.55 (3H, s), 1.97 (3H, s). HRMS (FAB) Calcd for $C_{23}H_{22}BrNO_4$: 456.0851. Found: 456.0831.

***N*-(5-Fluoro-2-phenoxyphenyl)-*N*-(5-methoxy-2-tri-*n*-butylstannylbenzyl)acetamide (10a)**. The oil **9a** (1.02 g, 2.30 mmol) was dissolved in dry toluene (20 mL) which had been degassed by bubbling nitrogen gas through it for 5 min. Tetrakis(triphenylphosphine)palladium (0) (266 mg, 230 μmol) and bis(tri-*n*-butyl)tin (1.16 mL, 2.31 mmol) were successively added. The reaction mixture was refluxed for 90 h under a nitrogen atmosphere. After cooling, the volatiles were evaporated under reduced pressure. The residue was chromatographed on silica gel with AcOEt/hexane (1/5) to afford **10a** (320 mg, 21%) as a yellowish oil. ^{1}H NMR ($CDCl_3$) δ: 7.10−7.34 (4H, m), 6.72−7.00 (7H, m), 5.25 (1H, d, J = 15.2 Hz), 4.37 (1H, d, J = 15.2 Hz), 3.70 (3H, s), 2.03 (3H, s), 1.18−1.43 (12H, m), 0.81−0.95 (15H, m). HRMS (FAB) Calcd for $C_{34}H_{46}FNO_3Sn$: 654.2489. Found: 654.2451.

***N*-(2,5-Dimethoxybenzyl)-*N*-(2-phenoxy-5-tri-*n*-butylstannylphenyl)acetamide (10b)**. The solid **9b** (584 mg, 1.5 mmol) was dissolved in dry toluene (10 mL) which had been degassed by bubbling nitrogen gas through it for 5 min. Tetrakis(triphenyphosphine)palladium (0) (173 mg, 150 μmol) and bis(tri-*n*-butyl)tin (0.76 mL, 1.51 mmol) were successively added. The reaction mixture was refluxed for 18 h under an argon atmosphere. After cooling, the volatiles were evaporated under reduced pressure. The residue was chromatographed on silica gel with AcOEt/hexane (1/5) to afford **10b** (450 mg, 45%) as a yellowish oil. ^{1}H NMR (300 MHz, $CDCl_3$) δ: 7.32 (1H, t, J = 7.8 Hz), 7.22 (1H, d, J = 7.9 Hz), 7.14 (1H, t, J = 7.3 Hz), 6.86−6.99 (5H, m), 6.81 (1H, d, J = 7.9 Hz), 6.62−6.71 (2H, m), 5.20 (1H, d, J = 14.5 Hz), 4.65 (1H, d, J = 14.5 Hz), 3.66 (3H, s), 3.50 (3H, s), 1.94 (3H, s), 1.25−1.51 (12H, m), 0.84−0.98 (15H, m). HRMS (FAB) Calcd for $C_{35}H_{49}NO_4Sn$: 666.2693. Found: 666.2726.

***N*-(5-Fluoro-2-phenoxyphenyl)-*N*-(2-iodo-5-methoxybenzyl)acetamide (3a)**. To a solution of **10a** (230 mg, 0.35 mmol) in CH_2Cl_2 (5 mL) was added iodine solid (260 mg, 1.0 mmol) in a dropwise manner at room temperature. The reaction mixture was stirred at room temperature for 3 h. After the reaction was completed, the saturated sodium metabisulfite solution was added until the color of the reaction mixture disappeared entirely. The organic layer was collected, and the reaction mixture was extracted with CH_2Cl_2 for a further two times. After the combined organic layer was washed with water and saturated NaCl solution and dried over Na_2SO_4, the solvent was removed to give a residue. The residue was chromatographed on silica gel with AcOEt/hexane (1/5) to give **3a** (140 mg, 81%) as a yellowish oil. HPLC determination: (1) 11.2 min; 3.9 mm ID × 150 mm, μ-Porasin (Waters); 1 mL/min, hexane/AcOEt, 9/1, UV at 254 nm. (2) 8.6 min; 4.6 mm ID × 250 mm, Capcell Pak C_{18} (SHISEIDO); 1.5 mL/min, CH_3CN/H_2O, 8/2, UV at 254 nm. ^{1}H NMR ($CDCl_3$) δ: 7.57 (1H, d, J = 8.6 Hz), 7.32 (2H, t, J = 7.9 Hz), 7.12 (1H, t, J = 7.3 Hz), 7.04 (1H, d, J = 2.9 Hz), 6.93−6.99 (1H, m), 6.80−6.89 (4H, m), 6.49 (1H, dd, J = 2.9, 8.6 Hz), 5.15 (1H, d, J = 15.1 Hz), 4.69 (1H, d, J = 15.1 Hz), 3.66 (3H, s), 2.00 (3H, s). Anal. ($C_{22}H_{19}FINO_3$) C, H, N. HRMS (FAB) Calcd for $C_{22}H_{19}FINO_3$: 492.0574. Found: 492.0523.

***N*-(2,5-Dimethoxybenzyl)-*N*-(5-iodo-2-phenoxyphenyl)acetamide (3b)**. To a solution of **10b** (300 mg, 0.45 mmol) in CH_2Cl_2 (5 mL) was added iodine solid (345 mg, 1.38 mmol) in a dropwise manner at room temperature. The reaction mixture was stirred at room temperature for 3 h. After the reaction was completed, the saturated sodium metabisulfite solution was added until the color of the reaction mixture disappeared. The organic layer was collected, and the reaction mixture was extracted with CH_2Cl_2 for further two times. After the combined organic layer was washed with water and saturated NaCl solution and dried over Na_2SO_4, the solvent was removed to give a residue. The residue was chromatographed on silica gel with AcOEt/hexane (1/5) to give **3b** (180 mg, 80%) as a white solid. HPLC determination: (1) 10.0 min; 3.9 mm ID × 150 mm, μ-Porasin (Waters); 1 mL/min, hexane/AcOEt, 9/1, UV at 254 nm. (2) 9.5 min; 4.6 mm ID × 250 mm, Capcell Pak C_{18} (SHISEIDO); 1.5 mL/min, CH_3CN/H_2O, 8/2, UV at 254 nm. Mp: 114.5−115.0 °C. ^{1}H NMR ($CDCl_3$) δ: 7.45 (1H, d, J = 8.6 Hz), 7.30−7.38 (3H, m), 7.14 (1H, t, J = 7.3 Hz), 6.95 (1H, d, J = 2.8 Hz), 6.84 (2H, d, J = 7.9 Hz), 6.66−6.75 (2H, m), 6.55 (1H, d, J = 8.6 Hz), 5.03 (1H, d, J = 14.3 Hz), 4.73 (1H, d, J = 14.3 Hz), 3.66 (3H, s), 3.56 (3H, s), 1.97 (3H, s). Anal. ($C_{23}H_{22}INO_4$) C, H, N. HRMS (FAB) Calcd for $C_{23}H_{22}INO_4$: 504.0672. Found: 504.0673.

***N*-(5-Fluoro-2-phenoxyphenyl)-*N*-(2-[^{131}I]iodo-5-methoxybenzyl)acetamide ([^{131}I]3a)**. Aqueous hydrogen peroxide (10 μL, 30% w/v) was added to a mixture of **10a** (100 μL, 1 mg/mL in ethanol), acetic acid (100 μL), and [^{131}I]NaI (18 MBq, 10 μL in 0.1M NaOH, specific activity: >30 GBq/μmol; Perkin-Elmer, Yokohama) in a sealed vial. The reaction was allowed to proceed for 30 min at room temperature, after which it was terminated by the addition of sodium metabisulfite (100 μL, 100 mg/mL in water). The reaction

mixture was injected onto a reverse-phase HPLC column (10 mm ID × 250 mm, HDS80 C_{18} (YMC); 4 mL/min, CH_3CN/H_2O, 9/1, UV at 254 nm). The fraction eluted at 11.4 min containing [^{131}I]**3a** was collected and evaporated with a nitrogen gas flow. The final product [^{131}I]**3a** was taken up in an isotonic saline solution (1 mL) and passed through a 0.22 μm filter into a sterile, pyrogen-free bottle with a radiochemical purity of >98% (10 MBq).

***N*-(2,5-Dimethoxybenzyl)-*N*-(5-[^{131}I]iodo-2-phenoxyphenyl)-acetamide** ([^{131}I]**3b**). Aqueous hydrogen peroxide (10 μL, 30% w/v) was added to a mixture of **10b** (100 μL, 1 mg/mL in ethanol), acetic acid (100 μL), and [^{131}I]NaI (18 MBq, 10 μL in 0.1M NaOH, specific activity: >30 GBq/μmol; Perkin-Elmer, Yokohama) in a sealed vial. The reaction was allowed to proceed for 30 min at room temperature, after which it was terminated by the addition of sodium metabisulfite (100 μL, 100 mg/mL in water). The reaction mixture was injected onto a reverse-phase HPLC column (10 mm ID × 250 mm, HDS80 C_{18} (YMC); 4 mL/min, CH_3CN/H_2O, 9/1, UV at 254 nm). The fraction eluted at 9.5 min containing [^{131}I]**3b** was collected and evaporated with a nitrogen gas flow. The final product [^{131}I]**3b** was taken up in an isotonic saline solution (1.0 mL) and passed through a 0.22 μm filter into a sterile, pyrogen-free bottle with a radiochemical purity of > 98% (8 MBq).

Identity Confirmation and Radiochemical Purity Determination. A solution of [^{131}I]**3a** or [^{131}I]**3b** (1 mL) containing nonradioactive **3a** or **3b** (1 mg/5 mL CH_3CN) was spotted on a silica gel TLC plate, which was then developed with AcOEt/hexane (1/1) as a mobile phase. The TLC plate was air-dried and placed in contact with a phosphor imaging plate (BAS-SR 127, Fuji Photo Film, Tokyo) for 10 min, and the radioactivity distribution on the plate was analyzed using a FUJI BAS 1800II bioimaging analyzer (Fuji Photo Film, Tokyo). [^{131}I]**3a** or [^{131}I]**3b** was identified by comparing the R_f with the nonradioactive **3a** (0.57) or **3b** (0.53), visualized by UV lamp at 254 nm.

Aliquots of the formulated solutions were used to establish chemical and radiochemical purity employing analytical HPLC (4.6 mm ID × 250 mm, LiChrosphor RP-18e (Merck); CH_3CN/H_2O, 7/3, UV at 254 nm). The retention times for [^{131}I]**3a** and [^{131}I]**3b** were 10.3 and 9.9 min at a flow rate of 1.0 mL/min, respectively.

In Vitro Binding Assays. Male Sprague−Dawley rats (n = 4) weighing 220−250 g were killed by decapitation under ether anesthesia, and their brains were quickly removed and frozen on powdered dry ice. Brain sagittal sections (20 μm) were cut on a cryostat microtome (HM560, Carl Zeiss, Germany) and thaw-mounted on glass slides (Matsunami Glass Ind., Tokyo), which were then dried at room temperature and stored at −18 °C until used for experiments. The brain sections were preincubated at 25 °C for 20 min in 50 mM Tris-HCl (pH 7.4) buffer. After preincubation, these sections were incubated at 37 °C for 30 min in the assay buffer containing [^{11}C]**1a** (1 nM, specific activity: 110 GBq/μmol), [^{11}C]-**2a** (1 nM, 50 GBq/μmol), or [^{11}C]flumazenil (1 nM, 210 GBq/μmol). To determine the IC_{50} values of **1a**, **2a**, **3a**, and **3b** for PBR) or CBR binding, brain sections were incubated with [^{11}C]ligands in the presence of increasing concentrations of the corresponding ligands (0.1 nM−1 μM). Nonradioactive **1a** and flumazenil (1 μM) were used to determine nonspecific bindings for PBR and CBR, respectively. After incubation, the sections were washed three times for 2 min each time with cold assay buffer, dipped in cold distilled water, and dried with warm air. These sections were then placed in contact with imaging plates (BAS-SR 127, Fuji Photo Film, Tokyo) for 60 min to analyze the distribution of their radioactivity with a FUJIX BAS 1800II bioimaging analyzer (Fuji). The region of interest (ROI) on the sections was placed on the cerebellum and the radioactivity in ROI was expressed as photostimulated-luminescence (PSL) values. PSL data corresponding to the radioactivity on the cerebellum in the presence and absence of the displaced ligand were determined. Specific binding for PBR or CBR was defined as total binding minus binding in the presence of **1a** or flumazenil (1 μM). The PSL data corresponding to specific binding at each compound concentration were calculated as percentages in relation to control specific bindings, which were converted to probit values to determine the IC_{50} of each compound.

Biodistribution Study. A saline solution of [^{131}I]3a or [^{131}I]3b (average of 0.5 MBq/100 μL), was injected into ddy mice (n = 3/[^{131}I]ligand; 30−40 g, 9 weeks, male, SLC, Shizuoka, Japan) through the tail vein. The animals were sacrificed by cervical dislocation at 1, 5, 15, 30, or 60 min after injection. The whole brain was quickly removed and bisected, and one-half was weighed. The radioactivity present in the brains was determined with a Packard autogamma scintillation counter. The percent dose per gram of brain (% dose/g) was calculated by comparison of the decay-corrected brain counts with the decay-corrected counts of suitably diluted aliquots of the injected material.

From another half brain, the cerebellum, olfactory bulb, striatum, hippocampus, thalamus, hypothalamus, and cerebral cortex were further dissected and weighed. The radioactivity present in these tissues was measured as described above.

Blocking Study. To determine in vivo specificity and selectivity of [^{131}I]3a binding to PBR, **1a** or **2a** at a dose of 1 mg/kg each was mixed with [^{131}I]3a (0.5 MBq/100 μL) and injected into ddy mice (n = 3; 30−40 g, 9 weeks, male, SLC, Shizuoka, Japan), respectively. At 30 min after injection, these mice were sacrificed by cervical dislocation and the whole brains were removed quickly. The brain tissue samples (cerebellum, olfactory bulb, striatum, hippocampus, thalamus, hypothalamus, and cerebral cortex) were dissected and treated as described above.

Ex Vivo Autoradiography. A saline solution of [^{131}I]**3a** (2 MBq/100 μL) was injected into a male Sprague−Dawley rat (220 g, 8 weeks, SLC, Shizuoka, Japan) through the tail vein. At 30 min after injection, the rat was sacrificed by decapitation under ether anesthesia. The brain was quickly removed and frozen on powdered dry ice. Brain sagittal sections (20 μm) were cut on a cryostat microtome (HM560), thaw-mounted on glass slides, and dried with warm air. These sections were then placed in contact with imaging plates (BAS-SR 127) for one week to analyze radioactivity distribution with a bioimaging analyzer. The radioactivity in the region of interest was expressed as photostimulated-luminescence (PSL) value per mm^2 region.

For the inhibition experiment, a mixture of [^{131}I]**3a** (2 MBq/100 μL) and **1a** (1 mg/kg, 10% EtOH in 200 μL saline) was used as described above.

In Vivo Stability of [^{131}I]3a in the Mouse Brains. After iv injection of [^{131}I]**3a** (0.2 MBq/100 μL) into ddy mice (n = 3), these mice were sacrificed by cervical dislocation at 30 min. The whole brain samples were removed quickly. The cerebellum and forebrain including the olfactory bulb were dissected from the mouse brain and homogenized together in an ice-cooled CH_3CN/H_2O (1/1, 1.0 mL) solution. The homogenate was centrifuged at 15 000 rpm for 10 min at 4 °C, and the supernatant was collected.

An aliquot of the supernatant (10 μL) containing trace of nonradioactive **3a** was spotted on a silica gel TLC plate, which was then developed with AcOEt/hexane (1/ 1) as a mobile phase. The TLC plate was air-dried and placed in contact with a phosphor imaging plate (BAS-SR 127) for 10 days, and the radioactivity distribution on the plate was analyzed using a FUJI BAS 1800II bioimaging analyzer. [^{131}I]**3a** was identified by comparing the R_f with the nonradioactive **3a** (0.57) visualized by UV lamp at 254 nm. The percent ratio of the unchanged [^{131}I]3a to the total radioactivity (corrected for decay) on the TLC chromatogram was calculated as % = (peak area for [^{131}I]**3a**/total radioactive peak area) × 100.

Acknowledgment. We thank Taisho Pharmaceutical Co., Ltd. (Tokyo, Japan) for providing DAA1106 (**1**).

Supporting Information Available: Elemental analyses, HPLC purities, and analytical HPLC charts, using reversed-phase and normal-phase solvents, of the target compounds. This material is available free of charge via the Internet at http://pubs.acs.org.

References

(1) "Peripheral-type Benzodiazepine Receptor" has been renamed as "Translocator Protein-18 (18kDa)": Papadopoulos, V.; Baraldi, M.; Guilarte, T.; Knudsen, T.; Lacapère, J.-J.; Lindemann, P.; Norenberg,

M. D.; Nutt, D.; Weizman, A.; Zhang, M.-R.; Gavish, M. Translocator Protein-18 (18kDa): New Nomenclature for the Peripheral-Type Benzodiazepine Receptor Based on its Structure and Molecular Function. *Trends Pharmacol. Sci*. **2006**, *27*, 402−409.

(2) Doble, A.; Ferris, O.; Burgevin, M. C.; Menager, J.; Uzan, A.; Dubroeucq, M. C.; Renault, C.; Gueremy, C.; Le Fur, G. Photoaffinity Labeling of Peripheral-type Benzodiazepine Binding Sites. *Mol. Pharmacol.* **1987**, *31*, 42−49.

(3) Anholt, R. R.; Pedersen, P. L.; DeSouza, E. B.; Snyder, S. H. The Peripheral-type Benzodiazepine Receptor: Localization to the Mitochondrial Outer Membrane. *J. Biol. Chem.* **1986**, *261*, 576−583.

(4) Culty, M.; Li, H.; Boujrad, N.; Bernassau, J. M.; Reversat, J. L.; Amri, H.; Vidic, B.; Papadopoulos, V. In Vitro Studies on the Role of the Peripheral Benzodiazepine Receptor in Steroidogenesis. *J. Steroid Biochem. Mol. Biol.* **1999**, *69*, 123−130.

(5) Braestrup, C.; Squires, R. F. Specific Benzodiazepine Receptors in Rat Brain Characterized by High Affinity [^{3}H]Dizaepam Binding. *Proc. Natl. Acad. Sci. U.S.A.* **1977**, *74*, 3805−3809.

(6) Benavides, J.; Quarteronet, D.; Imbault, F.; Malgouris, C.; Uzan, A.; Renault, C.; Dubroeucq, M. C.; Gueremy, C.; Le Fur, G. Labelling of "Peripheral-type" Benzodiazepine Binding Sites in the Rat Brain by Using [3H]PK 11195, an Isoquinoline Carboxamide Derivative: Kinetic Studies and Autoradiographic Localization. *J. Neurochem.* **1983**, *41*, 1744−1750.

(7) Anholt, R. R.; Murphy, K. M.; Mack, G. E.; Snyder, S. H. Peripheral-type Benzodiazepine Receptors in the Central Nervous System: Localization to Olfactory Nerves. *J. Neurosci.* **1984**, *4*, 593−603.

(8) Petit-Taboué, M. C.; Baron, J. C.; Barré, L.; Travère, J. M.; Speckel, D.; Camsonne, R.; MacKenzie, E. T. Brain Kinetics and Specific Binding of [^{11}C]PK 11195 to Omega3 Sites in Baboons: Positron Emission Tomography Study. *Eur. J. Pharmacol.* **1991**, *200*, 347−351.

(9) Rao, V. L.; Butterworth, R. F. Characterization of Binding Sites for the Omega3 Receptors Ligands [^{3}H]PK11195 and [^{3}H]Ro5-4864 in human brain. *Eur. J. Pharmacol.* **1997**, *340*, 89−90.

(10) Gavish, M.; Katz, Y.; Bar-Ami, S.; Weizman, R. Biochemical, Physiological and Pathological Aspects of the Peripheral Benzodiazepine Receptor. *J. Neurochem.* **1992**, *58*, 1589−1601.

(11) McGeer, P. L.; McGeer, E. G. The inflammatory Response System of Brain: Implications for Therapy of Alzheimer and Other Neurodegenerative Diseases. *Brain Res. Rev.* **1995**, *21*, 195−218.

(12) Benavides, J.; Fage, D.; Carter, C.; Scatton, B. Peripheral Type Benzodiazepine Binding Sites are a Sensitive Indirect Index of Neuronal Damage. *Brain Res.* **1987**, *421*, 167−172.

(13) Banati, R. B.; Myers, R.; Kreutzberg, G. W. PK ('peripheral benzodiazepine')-binding Sites in the CNS Indicate Early and Discrete Brain Lesions: Microautoradiographic Detection of [^{3}H]PK11195 Binding to Activated Microglia. *J. Neurocytol.* **1997**, *26*, 77−82.

(14) Banati, R. B.; Newcombe, J.; Gunn, R. N.; Cagnin, A.; Turkheimer, F.; Heppner, F.; Price, G.; Wegner, F.; Giovannoni, G.; Miller, D. H.; Perkin, G. D.; Smith, T.; Hewson, A. K.; Bydder, G.; Kreutzberg, G. W.; Jones, T.; Cuzner, M. L.; Myers, R. The Peripheral Benzodiazepine Binding Site in the Brain in Multiple Sclerosis: Quantitative In Vivo Imaging of Microglia as a Measure of Disease Activity. *Brain* **2000**, *123*, 2321−2337.

(15) Diorio, D.; Welner, S.; Butterworth, R.; Meaney, M.; Suranyl-Cadotte, R. Peripheral Benzodiazepine Binding Sites in Alzheimer's Disease Frontal Cortex and Temporal Cortex. *Neurobiol. Aging* **1991**, *12*, 255−258.

(16) Groom, G. N.; Junck, L.; Foster, N. L.; Frey, K. A.; Kuhl, D. E. PET of Peripheral Benzodiazepine Binding Sites in the Microgliosis of Alzheimer's Disease. *J. Nucl. Med.* **1995**, *36*, 2207−2210.

(17) Versijpt, J. J.; Dumont, F.; Van Laere, K. J.; Decoo, D.; Santens, P.; Audenaert, K.; Achten, E.; Slegers, G.; Dierckx, R. A.; Korf, J. Assessment of Neuroinflammation and Microglial Activation in Alzheimer's Disease with Radiolabelled PK11195 and Single Photon Emission Computed Tomography. A Pilot Study. *Eur. Neurol.* **2003**, *50*, 39−47.

(18) Sauvageau, A.; Desjardins, P.; Lozeva, V.; Rose, C.; Hazell, A. S.; Bouthillier, A.; Butterwort, R. F. Increased Expression of "Peripheral-type" Benzodiazepine Receptors in Human Temporal Lobe Epilepsy: Implications for PET Imaging of Hippocampal Sclerosis. *Metab. Brain Dis.* **2002**, *17*, 3−11.

(19) Mattner, F.; Katsifis, A.; Staykova, M.; Ballantyne, P.; Willenborg, D. O. Evaluation of a Radiolabelled Peripheral Benzodiazepine Receptor Ligand in the Central Nervous System Inflammation of Experimental Autoimmune Encephalomyelitis: a Possible Probe for Imaging Multiple Sclerosis. *Eur. J. Nucl. Med. Mol. Imaging* **2005**, *32*, 557−563.

(20) Camsonne, R.; Crouzel, C.; Comar, D.; Maziere, M.; Prenant, C.; Sastre, J.; Moulin, M. A.; Syrota, A. Synthesis of N-[^{11}C]-Methyl, N-(Methyl-1-propyl), (Chloro-2-phenyl)-1-isoquinoline Carboxamide-3 (PK11195): a New Ligand for Peripheral Benzodiazepine Receptors. *J. Labelled Compd. Radiopharm.* **1984**, *21*, 985−991.

(21) Cappelli, A.; Anzini, M.; Vomero, S.; De Benedetti, P. G.; Menziani, M. C.; Giorgi, G.; Manzoni, C. Mapping the Peripheral Benzodiazepine Receptor Binding Site by Conformationally Restrained Derivatives of 1-(2-Chlorophenyl)-1-*N*-methypropyl-3-isoquinolinecarboxamide (PK11195). *J. Med. Chem.* **1997**, *40*, 2910−2921.

(22) Matarrese, M.; Moresco, R. M.; Cappelli, A.; Anzini, M.; Vomero, S.; Simonelli, P.; Verza, E.; Magni, F.; Sudati, F.; Soloviev, D.; Todde, S.; Carpinelli, A.; Kienle, M. G.; Fazio, F. Labeling and Evaluation of N-[^{11}C]Methylated Quinoline-2-carboxamides as Potential Radioligands for Visualization of Peripheral Benzodiazepine Receptors. *J. Med. Chem.* **2001**, *44*, 579−585.

(23) Gulyas, B.; Halldin, C.; Vas, A.; Banati, R. B.; Shchukin, E.; Finnema, S.; Tarkainen, J.; Tihanyi, K.; Szilagyi, G.; Farde, L. [^{11}C]-Vinpocetine: a Prospective Peripheral Benzodiazepine Receptor Ligand for Primate PET Studies. 1: *J. Neurol. Sci.* **2005**, *229*−*230*, 219−223.

(24) Zhang, M.-R.; Ogawa, M.; Maeda, J.; Ito, T.; Noguchi, J.; Kumata, K.; Okauchi T.; Suhara, T.; Suzuki, K. [2-^{11}C]Isopropyl-, [1-^{11}C]-Ethyl- and [^{11}C]Methyl- Labeled Phenoxyphenyl Acetamide Derivatives as PET Ligands for Peripheral Benzodiazepine Receptor: Radiosynthesis, Uptake and In Vivo Binding in Brain. *J. Med. Chem.* **2006**, *49*, 2735−2742.

(25) Zhang, M.-R.; Kida, T.; Noguchi, J.; Furutsuka, K.; Maeda, J.; Suhara, T.; Suzuki, K. [^{11}C]DAA1106: Radiosynthesis and *In Vivo* Binding to Peripheral Benzodiazepine Receptors in Mouse Brain. *Nucl. Med. Biol.* **2003**, *30*, 513−519.

(26) Maeda, J.; Suhara, T.; Zhang, M.-R.; Okauchi, T.; Yasuno, F.; Ikoma, Y.; Inaji, M.; Nagai, Y.; Ichimiya; Ohbayashi, S.; Suzuki, K. Novel Peripheral Benzodiazepine Receptor Ligand [^{11}C]DAA1106 for PET; an Imaging Tool for Glial Cells in the Brain. *Synapse* **2004**, *52*, 283−291.

(27) Zhang, M.-R.; Maeda, J.; Ogawa, M.; Noguchi, J.; Ito, T.; Yoshida, Y.; Okauchi, T.; Obayashi, S.; Suhara, T.; Suzuki, K. Devlopment of a New Radioligand, N-(5-Fluoro-2 phenoxyphenyl)-N-(2-[^{18}F]-fluoroethoxyl-5-methoxybenzyl)acetamide, for PET Imaging of Peripheral Benzodiazepine Receptor in Primate Brain. *J. Med. Chem.* **2004**, *47*, 2228−2235.

(28) Chaki, S.; Funakoshi, T.; Yoshikawa, R.; Okuyama, S.; Okubo, T.; Nakazato, A.; Nagamine, M.; Tomisawa, K. Binding Characteristics of [^{3}H]DAA1106, a Novel and Selective Ligand for Peripheral Benzodiazepine Receptors. *Eur. J. Pharmacol.* **1999**, *371*, 197−204.

(29) Culty, M.; Silver, P.; Nakazato, A.; Gazouli, M.; Li, H.; Muramatsu, M.; Okuyama, S.; Papadopoulos, V. Peripheral Benzodiazepine Receptor Binding Properties and Effects on Steroid Synthesis of Two New Phenoxy Phenylacetamide Derivatives, DAA1097 and DAA1106. *Drug Dev. Res.* **2001**, *52*, 475−484.

(30) Okubo, T.; Yoshikawa, R.; Chaki, S.; Okuyama, S.; Nakazato, A. Design, Synthesis and Structure-affinity Relationships of Aryloxyanilide Derivatives as Novel Peripheral Benzodiazepine Receptor Ligands. *Bioorg. Med. Chem.* **2004**, *12*, 423−438.

(31) Fujimura, Y.; Ikoma, Y.; Yasuno, F.; Suhara, T.; Ota, M.; Matsumoto, R.; Maeda, J.; Nazaki, S.; Takano, A.; Kosaka, J.; Zhang, M.-R.; Nakao, R.; Toyama, H.; Suzuki, K.; Kato, N.; Ito, H. Quantitative Analyses of [^{18}F]FEDAA1106 Binding to Peripheral Benzodiazepine Receptors in Living Human Brain. *J. Nucl. Med.* **2006**, *47*, 43−50.

(32) Ikoma, Y.; Yasuno, F.; Ito, H.; Suhara, T.; Ota, M.; Toyama, H.; Fujimura, Y.; Takano, A.; Maeda, J.; Zhang, M.-R.; Nakao, R.; Suzuki, K. Quantitative Analysis for Estimating Binding Potential of the Peripheral Benzodiazepine Receptor with [(11)C]DAA1106. *J. Cereb. Blood Flow. Metab.* **2006**, in press.

(33) Gildersleeve, D. L.; Van Dort, M. E.; Johnson, J. W.; Sherman, P. S.; Wieland, D. M. Synthesis and Evaluation of [^{123}I]-Iodo-PK11195 for Mapping Peripheral-type Benzodiazepine Receptors (omega 3) in Heart. 1. *Nucl. Med. Biol.* **1996**, *23*, 23−28.

(34) Homes, T. P.; Mattner, F.; Keller, P. A.; Katsifis, A. Synthesis and In Vitro Binding of N,N-Dialkyl-2-phenylindol-3-yl-glyoxylamides for the Peripheral Benzodiazepine Binding Sites. *Bioorg. Med. Chem.* **2006**, *14*, 3938−3946.

(35) Mattner, F.; Mardon, K.; Loc'h, C.; Katsifis, A. Pharmacological Evaluation of an [(123)I] Labelled Imidazopyridine-3-acetamide for the Study of Benzodiazepine Receptors. *Life Sci.* **2006**, *79*, 287−294.

(36) Okubo, T.; Yoshikawa, R.; Chaki, S.; Okuyama, S.; Nakazato, A. Design, Synthesis and Structure-affinity Relationships of Aryloxyanilide Derivatives as Novel Peripheral Benzodiazepine Receptor Ligands. *Bioorg. Med. Chem.* **2004**, *12*, 423−438.

JM061127N